

See discussions, stats, and author profiles for this publication at: <https://www.researchgate.net/publication/281467630>

Artifacts in Absorption Measurements of Organometal Halide Perovskite Materials: What Are the Real Spectra?

ARTICLE in JOURNAL OF PHYSICAL CHEMISTRY LETTERS · SEPTEMBER 2015

Impact Factor: 7.46 · DOI: 10.1021/acs.jpclett.5b01406

CITATION

1

READS

65

2 AUTHORS:



Yuxi Tian

Nanjing University

38 PUBLICATIONS 596 CITATIONS

SEE PROFILE



Ivan G Scheblykin

Lund University

80 PUBLICATIONS 1,498 CITATIONS

SEE PROFILE

Artifacts in Absorption Measurements of Organometal Halide Perovskite Materials: What Are the Real Spectra?

ABSTRACT: Organometal halide (OMH) perovskites have attracted lots of attention over the last several years due to their very promising performance as the materials for solar cells and light-emitting devices. Photophysical processes in these hybrid organic–inorganic semiconductors are still heavily debated. To know precise absorption spectra is absolutely necessary for quantitative understanding of the fundamental properties of OMH perovskites. We show that to measure the absorption of perovskite materials correctly is a difficult task which could be easily overlooked by the community. Many of the published absorption spectra exhibit a characteristic step-like featureless shape due to light scattering, high optical density of individual perovskite crystals and poor coverage of the substrate. We show how to recognize these artifacts, to avoid them, and to use absorption spectra of films for estimation of the surface coverage ratio.

Organometal halide (OMH) perovskites have attracted broad interest in the past years.^{1,2} Broad absorption range, high absorption coefficient, fast charge separation, slow charge recombination as well as high charge mobility^{3–7} make OHM perovskites optimistic candidates as materials for low-cost efficient solar cells and light-emitting devices.^{8–12} In spite of very high solar cell power conversion efficiencies, the devices suffer from chemical and morphological instability.^{13–15} The material itself is prone to photo and environmentally induced chemical reactions that may change its properties even during measurements.^{7,16–18} In addition to this, inhomogeneity of the OMH perovskite films at nano- and micrometer scale makes quantitative optical measurements difficult.

Inhomogeneities of the films are often inherent to the preparation procedures. The device performance have shown to be strongly dependent on the preparation method.^{1,3,4,19–22} Although solution processability of OMH perovskite is an advantage for applications, it causes great uncertainty of the final crystalline material. Perovskite samples prepared by spin-casting from an equimolar mixture of the methylammonium iodide and lead iodide precursors in γ -butyrolactone are actually not uniform films but consist of many isolated islands as reported^{8,16,23} and shown in Figure 1b. Such inhomogeneity of the film, if not taken into account, can affect the optical measurements like steady-state and time-resolved absorption spectroscopy leading to data misinterpretation. Absorption spectroscopy has been routinely used to obtain fundamental information on excited states in perovskites.^{1,3,24–30} However, the effect of sample inhomogeneity must be taken into account in such measurements.

A featureless, flat, step-like spectrum has almost nothing to do with the spectrum of the OMH perovskite material itself.

When the surface is not fully covered, most of the light just passes unattenuated through the blank area where no perovskite material exists. Conversely, for the perovskite “islands”, the optical density is often so large that most of the light is absorbed. As a result, the overall optical density of the sample measured by an ordinary absorption spectrometer is moderate

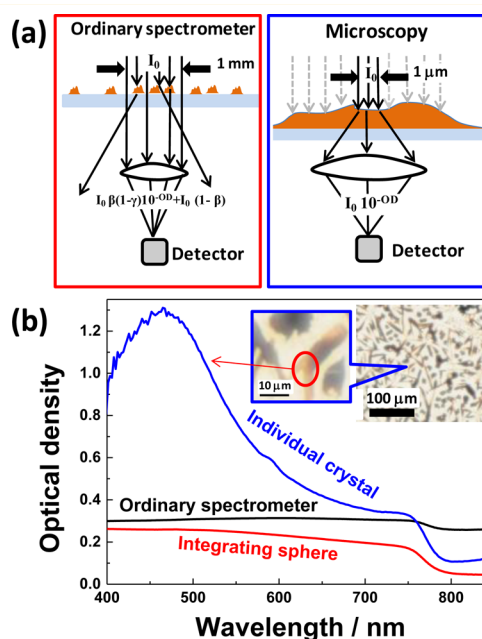


Figure 1. (a) Cartoon illustrating light penetration through the perovskite sample and detection by an ordinary spectrometer (low collection efficiency) and an optical microscope (high collection efficiency and spatial resolution). (b) Absorption spectra measured by the ordinary spectrometer, the spectrometer with integrating sphere and the microscope. The crystal whose spectrum was measured by the microscope is marked by the red circle.

($0.2 < \text{optical density (OD)} < 1$), which is usually interpreted as good conditions for absorption measurements. Neutral (gray) color semitransparent perovskite solar cells have their appearance because of this effect.³¹ However, such an absorption spectrum has almost nothing to do with the absorption of the material itself: it shows almost constant optical density in almost the whole visible region and an abrupt drop in the region of the semiconductor bandgap (black line in Figure 1b). Spectra looking like that can be seen in many publications.^{3,18,25,30}

Received: July 3, 2015

Accepted: August 17, 2015

Published: September 3, 2015



Another obvious and important effect originated from the inhomogeneity is light scattering, which leads to extra loss of the incident light resulting in increasing of the overall attenuation of the incoming light and also deforming the spectrum. Poor coverage, large optical density of individual crystals and light scattering are the most likely reasons that the reported absorption coefficient of OMH perovskites varies a lot when reported by different groups.^{1,4,32} We herein rationalize the absorption spectra of $\text{CH}_3\text{NH}_3\text{PbI}_3$ samples deposited on glass with incomplete coverage.

To investigate this issue experimentally and theoretically, we measured the absorption spectra of a $\text{CH}_3\text{NH}_3\text{PbI}_3$ perovskite film using an ordinary absorption spectrometer, an absorption spectrometer equipped integrating sphere detector and an optical microscope (Figure 1b). The film was prepared by surface deposition using an equimolar solution of lead iodide (PbI_2) and methylammonium iodide ($\text{CH}_3\text{NH}_3\text{I}$) in γ -butyrolactone as previously described¹⁶ (see Supporting Information for details). As the optical microscopy image in Figure 1b shows, this sample preparation method results in samples with random crystals only partially covering the surface.

Absorption spectrum of the perovskite film obtained using an ordinary absorption spectrometer is shown in Figure 1b by black line. The spectrum shows a step-like featureless shape (constant OD above the bandgap) with high background in the NIR region where no absorption of perovskite material is expected. By using an integrating sphere (red line in Figure 1b), the background in the NIR region is significantly reduced and the band edge can be clearly seen. However, it is still almost "flat" (OD is still only slightly wavelength dependent above the bandgap) all over the visible range without any features. This spectrum is similar to some of the reported spectra.^{3,18} The blue line in Figure 1b shows the absorption spectrum of an individual crystal measured by an optical microscope. The background in the NIR region reduces and becomes comparable with that for spectrum measured by integrating sphere. Contrary to the both spectra measured by the spectrometer, clear features with relatively high light absorption can be seen in the visible range.

A UV–vis absorption spectrometer cannot correctly measure the absorption of the material if the material does not fully cover the surface.

To understand the origin of such differences in the spectral shapes, let us write the intensity of light transmitted through the sample that is depicted in Figure 1a

$$I = I_0\beta(1 - \gamma(\lambda))10^{-\text{OD}(\lambda)} + I_0(1 - \beta) \quad (1)$$

Then the optical density measured by an ordinary spectrometer is

$$A_{\text{measured}} = -\log[\beta(1 - \gamma(\lambda))10^{-\text{OD}(\lambda)} + (1 - \beta)] \quad (2)$$

where I_0 is the intensity of the incident light; OD is the optical density of individual perovskite particles; β is the substrate coverage ratio \equiv (area covered by perovskite)/(total area), $\beta = 1$ for a continuous film; and γ is the scattering coefficient ($\gamma = 0$, no scattering, $\gamma = 1$, all light coming to the particle is scattered).

Scattering on particles of much larger in size than λ (which is the case for the perovskite sample presented in Figure 1b) is only weakly wavelength-dependent. Such scattering can be seen as a deviation of the light propagation direction due to refraction and reflection inside the perovskite crystals. Because the light collection optics of an ordinary absorption spectrometer has a very low numerical aperture, only light propagated very close to the direction of the incident light is collected and measured. That is why the larger scattering, the smaller the measured transmission.

High background below the band gap ($\lambda > 800$ nm) is the characteristic feature of light scattering by large micrometer-sized OMH perovskite particles.

Using an integrating sphere detector in the absorption spectrometer allows collecting most of the scattered light and reducing the spectral artifacts related to scattering substantially. The spectrum shown in Figure 1b (red line) possesses a quite small offset in the NIR region but still has the step-like shape and a very low optical density (0.3) due to the low surface coverage.

How can one get rid of the influence of the light directly transmitted by uncovered area of the sample? First of all, one could just prepare an optically thin perovskite film with 100% coverage ($\beta = 1$); however, this is not always easy to do for many perovskite preparation methods. Often, when good coverage is obtained, the optical density of the films is too large to measure it accurately or to use in precise optical experiments. Another approach is to measure absorption of an individual crystal. This is what we did using an optical microscope and a tungsten lamp (Figure 1a). The spectrum of the lamp was measured when the light was coming through several micrometer sized crystals and though an uncovered part of the substrate. Decimal logarithm of the ratio of the two signals gives the optical density shown in Figure 1b by the blue line. The result is quite impressive, the difference from the spectra obtained using the absorption spectrometer is very large (Figure 1b).

Optical density of the individual crystal close to the band gap at 700 nm was 2 times larger than measured with the integrating sphere detector and 6 times more at 470 nm. It turns out that the spectrum possesses the shape that was almost totally invisible in the spectra obtained using absorption spectrometers (compare black and red lines in Figure 1b).

To illustrate how the real spectrum of a perovskite crystal transforms to the step-like featureless spectrum measured by standard spectrometers, we checked the effect from coverage ratio, optical density of the crystals and scattering using eq 2, where for $\text{OD}(\lambda)$ we used the experimental spectrum of the individual crystal with subtracted background ($A_{\text{ind}}(\lambda)$, shown in Figure 1b by blue line). By subtracting the constant background of 0.1, we removed the wavelength independent component of the light scattering. Light scattering still influences the microscopy measurement because the objective lens even with high numerical aperture cannot collect the scattered light completely.

The effect of the coverage is shown in Figure 2. As one can see, when the sample is fully covered with crystals ($\beta = 1$), one can get the correct absorption spectrum by an ordinary spectrometer. When the coverage ratio decreases, the spectrum

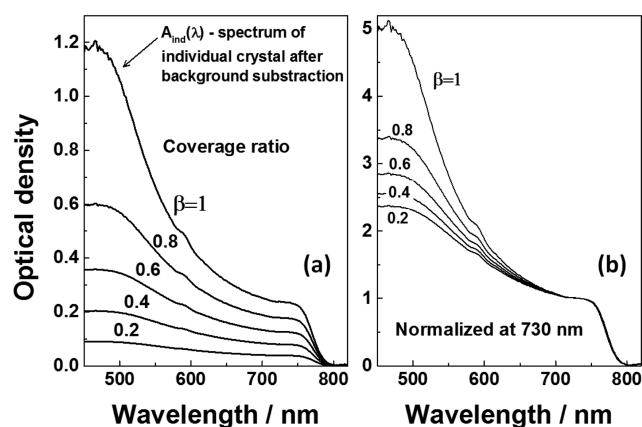


Figure 2. Effect of the coverage ratio β on the absorption spectrum.

flattens down and starts looking like a step. A clear comparison of the spectral shape can be seen in Figure 2b after normalizing the spectra at 730 nm. It is important to note that the variation of the coverage ratio as such does not influence the observed position of the band edge (Figure 2 b).

Detection by integrating sphere in the UV/vis takes care of the scattering problem but not the problem of incomplete surface coverage.

Figure 3 shows how the optical density of individual crystals can affect the absorption spectrum. A coverage ratio $\beta = 0.5$ is used for the calculation. To change the thickness of the individual crystals, we just multiplied the experimentally measured spectrum $A_{\text{ind}}(\lambda)$ with a coefficient ξ , which was varied from 0.5 to 8. As one can see, upon increasing of the crystal thickness (parameter ξ) the spectrum transforms to the featureless step-like “flat” spectrum. The last curve ($\xi = 8$) corresponds to the optical density of individual crystals at 730 nm (close to the band edge) of 1.6. Using the published value of the Napierian absorption coefficient ($\alpha \approx 30\,000\text{ cm}^{-1}$ at 730 nm),⁴ we estimate the thickness of the crystals with $\xi = 8$ to be $1.2\text{ }\mu\text{m}$. So, it is important to note that in samples with incomplete coverage increasing of the optical density of the individual crystals (increasing of the crystals thickness of more than 500 nm which is the typical value for perovskite solar cells) noticeably shifts the apparent band edge toward longer wavelengths (Figure 3 b). This effect should be taken into account when the band edge energy is determined from an experimental absorption spectrum.

Light scattering also leads to flattening of the spectrum (Figure 4), but it does not shift the observed band edge. The characteristic feature of the light scattering on large particles is high detected background absorption below the band edge ($\lambda > 800\text{ nm}$).

Using the eq 2 and the measured spectrum of the individual crystal we were able to satisfactory fit the experimental spectrum measured using integrating sphere (Figure 5). The parameters of the fit are coverage ratio $\beta = 0.45$, scattering coefficient $\gamma = 0.23$, optical density of individual crystals $\xi A_{\text{ind}}(\lambda)$, where $A_{\text{ind}}(\lambda)$ is the spectrum of the individual crystal measured experimentally with background subtraction and

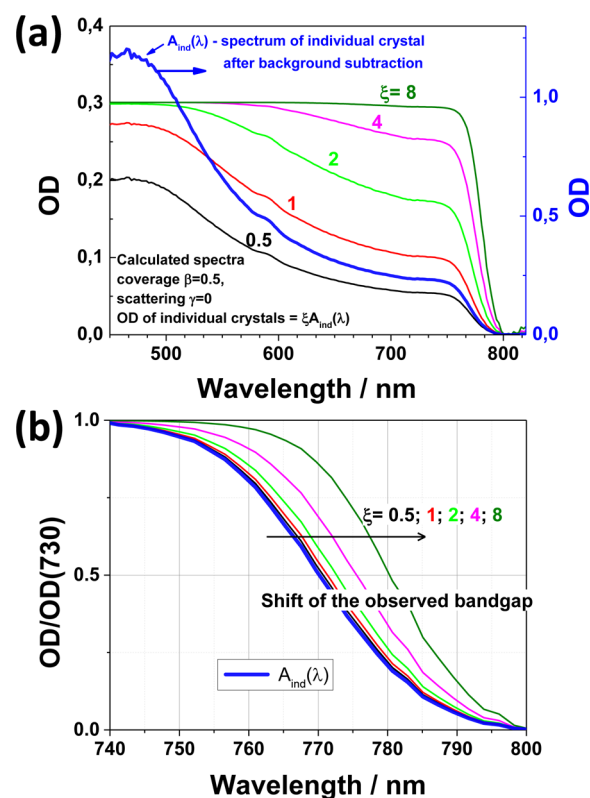


Figure 3. Effect of the optical density of individual crystals on the absorption spectrum, 50% of the surface is covered by the crystals. A clear shift of the apparent band edge is observed. The crystals' thickness in calculations was varied from about 80 nm to $1.2\text{ }\mu\text{m}$ (parameter ξ from 0.5 to 8).

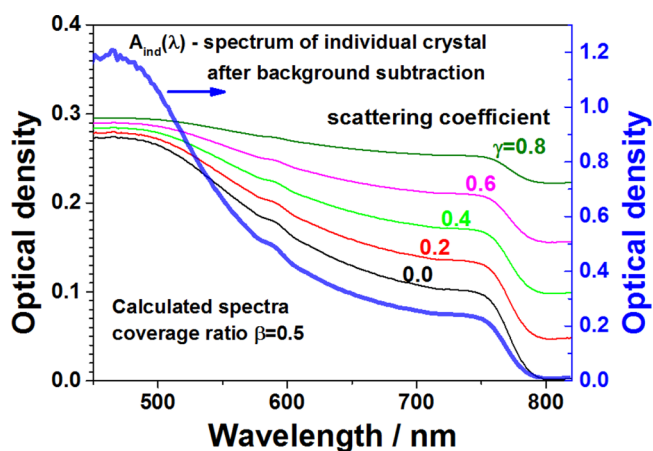


Figure 4. Effect of light scattering on the absorption spectrum.

$\xi = 2.3$ is the thickness scaling factor. The fact that to fit the spectrum we needed to increase the optical density of the crystals by the factor of $\xi = 2.3$ in comparison to the experimentally measured is not a surprise. This is because, as one can see from the microphotograph of the sample (Figure 1b), most of the crystals possess a much higher optical density than the one we measured.

There is still an obvious discrepancy between the measured and calculated spectra in the region of the band edge. We relate it to possible inhomogeneity of absorption spectra of individual crystals, this effect needs further investigation.

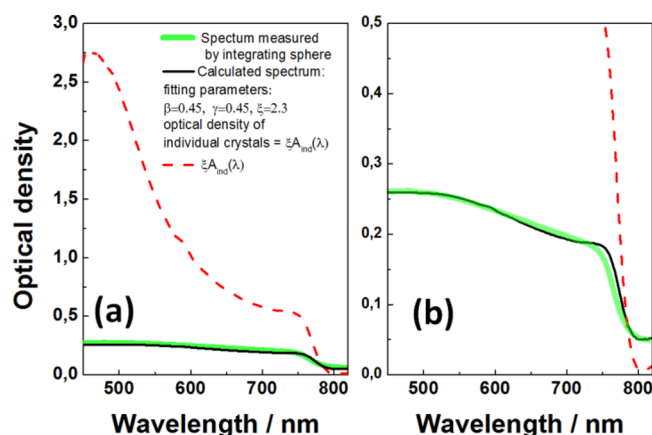


Figure 5. (a) Fit of the experimental spectrum by integrating sphere using the spectrum of the individual crystal. (b) Same graph as in (a) in different scale.

Preparation of homogeneous optically clean and transparent films could directly avoid the artifacts in absorption because their origin is in the poor coverage ratio, high optical density of individual crystals, and light scattering. The coverage ratio and the homogeneity of the film strongly depend on the sample preparation methods. Literature data shows that spin-casting perovskite precursor solutions directly on glass substrates often produce inhomogeneous films possessing “flat” step-like absorption spectra.^{3,18} The homogeneity of the films can be improved by spin-casting the solution onto different surfaces or using other methods like dual source evaporation, which thus lead to correct absorption spectrum measurement.^{32,33}

Thick OMH perovskite films with incomplete coverage can possess an apparent red-shift of the band edge by several nanometers—a pure optical effect.

In conclusion, we showed that to measure the absorption spectrum of organometal halide perovskite materials is not a trivial task due to poor surface coverage, high optical density of individual crystals, and light scattering. Many of the published spectra of perovskite films show almost constant optical density over the whole visible region which reflects the overall light transmission of the samples but not the absorption ability of the materials. Moreover, high optical density of individual crystals shifts the observed band edge position toward longer wavelengths by several nanometers or more. Although using an integrating sphere for transmitted light detection reasonably removes the effect of light scattering, the effect of poor coverage can be eliminated only by measuring the absorption of individual perovskite crystals. It is worth noting that these factors affect not only the steady-state but also the transient absorption measurements that are crucial for understanding ultrafast excited state processes. Here, we presented a spectrum of an individual micrometer-sized perovskite crystals measured by an optical microscope, which shows that the absorption coefficient in the region of 450 nm can be significantly underestimated by routine absorption measurements. We observed indications of inhomogeneity of perovskite absorption spectra at the level of individual crystals. Having the correct

material spectrum and the spectrum of a film, one can assess the surface coverage ratio for the film using the proposed model.

Yuxi Tian

Ivan G. Scheblykin*

Chemical Physics, Lund University, P.O. Box 124,
SE-22100 Lund, Sweden

■ ASSOCIATED CONTENT

Supporting Information

The Supporting Information is available free of charge on the ACS Publications website at DOI: 10.1021/acs.jpclett.5b01406.

Experimental section. (PDF)

■ AUTHOR INFORMATION

Corresponding Author

*E-mail: Ivan.Sheblykin@chemphys.lu.se.

Notes

The authors declare no competing financial interest.

■ ACKNOWLEDGMENTS

We thank Dr. Mohamed Abdellah for providing us the $\text{CH}_3\text{NH}_3\text{PbI}_3$ stock solution and Dr. Eva Unger and Dr. Arkady Yartsev for valuable discussions. This study was financially supported by the Swedish Research Council, the Knut & Alice Wallenberg Foundation and the Crafoord Foundation.

■ REFERENCES

- (1) Green, M. A.; Ho-Baillie, A.; Snaith, H. J. The Emergence of Perovskite Solar Cells. *Nat. Photonics* **2014**, *8*, 506–514.
- (2) Snaith, H. J. Perovskites: The Emergence of a New Era for Low-Cost, High-Efficiency Solar Cells. *J. Phys. Chem. Lett.* **2013**, *4*, 3623–3630.
- (3) Stranks, S. D.; Eperon, G. E.; Grancini, G.; Menelaou, C.; Alcocer, M. J. P.; Leijtens, T.; Herz, L. M.; Petrozza, A.; Snaith, H. J. Electron-Hole Diffusion Lengths Exceeding 1 Micrometer in an Organometal Trihalide Perovskite Absorber. *Science* **2013**, *342*, 341–344.
- (4) Xing, G.; Mathews, N.; Sun, S.; Lim, S. S.; Lam, Y. M.; Grätzel, M.; Mhaisalkar, S.; Sum, T. C. Long-Range Balanced Electron- and Hole-Transport Lengths in Organic-Inorganic $\text{CH}_3\text{NH}_3\text{PbI}_3$. *Science* **2013**, *342*, 344–347.
- (5) Ponseca, C. S.; Savenije, T. J.; Abdellah, M. A.; Zheng, K.; Yartsev, A. P.; Pascher, T.; Harlang, T.; Chabera, P.; Pullerits, T.; Stepanov, A.; et al. Organometal Halide Perovskite Solar Cell Materials Rationalized – Ultrafast Charge Generation, High and Microsecond-Long Balanced Mobilities and Slow Recombination. *J. Am. Chem. Soc.* **2014**, *136*, 5189–5192.
- (6) Savenije, T. J.; Ponseca, C. S.; Kunneman, L.; Abdellah, M.; Zheng, K.; Tian, Y.; Zhu, Q.; Canton, S. E.; Scheblykin, I. G.; Pullerits, T.; et al. Thermally Activated Exciton Dissociation and Recombination Control the Carrier Dynamics in Organometal Halide Perovskite. *J. Phys. Chem. Lett.* **2014**, *5*, 2189–2194.
- (7) Stranks, S. D.; Burlakov, V. M.; Leijtens, T.; Ball, J. M.; Goriely, A.; Snaith, H. J. Recombination Kinetics in Organic-Inorganic Perovskites: Excitons, Free Charge, and Subgap States. *Phys. Rev. Appl.* **2014**, *2*, 034007.
- (8) Kim, H.-S.; Lee, C.-R.; Im, J.-H.; Lee, K.-B.; Moehl, T.; Marchioro, A.; Moon, S.-J.; Humphry-Baker, R.; Yum, J.-H.; Moser, J. E.; et al. Lead Iodide Perovskite Sensitized All-Solid-State Submicron Thin Film Mesoscopic Solar Cell with Efficiency Exceeding 9%. *Sci. Rep.* **2012**, *2*, 591.
- (9) Tan, Z.-K.; Moghaddam, R. S.; Lai, M. L.; Docampo, P.; Higler, R.; Deschler, F.; Price, M.; Sadhanala, A.; Pazos, L. M.; Credgington,

D.; et al. Bright Light-Emitting Diodes Based on Organometal Halide Perovskite. *Nat. Nanotechnol.* **2014**, *8*, 737–743.

(10) D'Innocenzo, V.; Srimath Kandada, A. R.; De Bastiani, M.; Gandini, M.; Petrozza, A. Tuning the Light Emission Properties by Band Gap Engineering in Hybrid Lead Halide Perovskite. *J. Am. Chem. Soc.* **2014**, *136*, 17730–17733.

(11) Deschler, F.; Price, M.; Pathak, S.; Klintberg, L.; Jarausch, D. D.; Higler, R.; Huettner, S.; Leijtens, T.; Stranks, S. D.; Snaith, H. J.; et al. High Photoluminescence Efficiency and Optically-Pumped Lasing in Solution-Processed Mixed Halide Perovskite Semiconductors. *J. Phys. Chem. Lett.* **2014**, *5*, 1421–1426.

(12) Zhou, H.; Chen, Q.; Li, G.; Luo, S.; Song, T. -b.; Duan, H.-S.; Hong, Z.; You, J.; Liu, Y.; Yang, Y. Interface Engineering of Highly Efficient Perovskite Solar Cells. *Science* **2014**, *345*, 542–546.

(13) Christians, J. A.; Miranda Herrera, P. A.; Kamat, P. V. Transformation of the Excited State and Photovoltaic Efficiency of $\text{CH}_3\text{NH}_3\text{PbI}_3$ Perovskite upon Controlled Exposure to Humidified Air. *J. Am. Chem. Soc.* **2015**, *137*, 1530–1538.

(14) Guarnera, S.; Abate, A.; Zhang, W.; Foster, J. M.; Richardson, G.; Petrozza, A.; Snaith, H. J. Improving the Long-Term Stability of Perovskite Solar Cells with a Porous Al_2O_3 Buffer-Layer. *J. Phys. Chem. Lett.* **2015**, *6*, 432–437.

(15) Niu, G.; Guo, X.; Wang, L. Review of Recent Progress in Chemical Stability of Perovskite Solar Cells. *J. Mater. Chem. A* **2014**, *3*, 8970–8980.

(16) Tian, Y.; Merdasa, A.; Peter, M.; Abdellah, M.; Zheng, K.; Ponseca, C. S.; Pullerits, T.; Yartsev, A.; Sundstrom, V.; Scheblykin, I. G. Giant Photoluminescence Blinking of Perovskite Nanocrystals Reveals Single-Trap Control of Luminescence. *Nano Lett.* **2015**, *15*, 1603–1608.

(17) Unger, E. L.; Hoke, E. T.; Bailie, C. D.; Nguyen, W. H.; Bowring, A. R.; Heumuller, T.; Christoforo, M. G.; McGehee, M. D. Hysteresis and Transient Behavior in Current-Voltage Measurements of Hybrid-Perovskite Absorber Solar Cells. *Energy Environ. Sci.* **2014**, *7*, 3690–3698.

(18) Galisteo-Lopez, J. F.; Anaya, M.; Calvo, M. E.; Miguez, H. Environmental Effects on the Photophysics of Organic-Inorganic Halide Perovskites. *J. Phys. Chem. Lett.* **2015**, *6*, 2200–2205.

(19) Chen, Q.; Zhou, H.; Hong, Z.; Luo, S.; Duan, H.-S.; Wang, H.-H.; Liu, Y.; Li, G.; Yang, Y. Planar Heterojunction Perovskite Solar Cells via Vapor-Assisted Solution Process. *J. Am. Chem. Soc.* **2014**, *136*, 622–625.

(20) Pathak, S.; Sepe, A.; Sadhanala, A.; Deschler, F.; Haghighirad, A.; Sakai, N.; Goedel, K. C.; Stranks, S. D.; Noel, N.; Price, M.; et al. Atmospheric Influence upon Crystallization and Electronic Disorder and Its Impact on the Photophysical Properties of Organic-Inorganic Perovskite Solar Cells. *ACS Nano* **2015**, *9*, 2311–2320.

(21) Shi, J.; Wei, H.; Lv, S.; Xu, X.; Wu, H.; Luo, Y.; Li, D.; Meng, Q. Control of Charge Transport in the Perovskite $\text{CH}_3\text{NH}_3\text{PbI}_3$ Thin Film. *ChemPhysChem* **2015**, *16*, 842–847.

(22) Yamada, Y.; Nakamura, T.; Endo, M.; Wakamiya, A.; Kanemitsu, Y. Photocarrier Recombination Dynamics in Perovskite $\text{CH}_3\text{NH}_3\text{PbI}_3$ for Solar Cell Applications. *J. Am. Chem. Soc.* **2014**, *136*, 11610–11613.

(23) He, M.; Zheng, D.; Wang, M.; Lin, C.; Lin, Z. High Efficiency Perovskite Solar Cells: From Complex Nanostructure to Planar Heterojunction. *J. Mater. Chem. A* **2014**, *2*, 5994–6003.

(24) Gamliel, S.; Etgar, L. Organometal Perovskite Based Solar Cells: Sensitized versus Planar Architecture. *RSC Adv.* **2014**, *4*, 29012.

(25) Eperon, G. E.; Stranks, S. D.; Menelaou, C.; Johnston, M. B.; Herz, L. M.; Snaith, H. J. Formamidinium Lead Trihalide: A Broadly Tunable Perovskite for Efficient Planar Heterojunction Solar Cells. *Energy Environ. Sci.* **2014**, *7*, 982.

(26) Chiang, Y.-F.; Jeng, J.-Y.; Lee, M.-H.; Peng, S.-R.; Chen, P.; Guo, T.-F.; Wen, T.-C.; Hsu, Y.-J.; Hsu, C.-M. High Voltage and Efficient Bilayer Heterojunction Solar Cells Based on an Organic-Inorganic Hybrid Perovskite Absorber with a Low-Cost Flexible Substrate. *Phys. Chem. Chem. Phys.* **2014**, *16*, 6033–6040.

(27) D'Innocenzo, V.; Grancini, G.; Alcocer, M. J. P.; Kandada, A. R. S.; Stranks, S. D.; Lee, M. M.; Lanzani, G.; Snaith, H. J.; Petrozza, A. Excitons versus Free Charges in Organo-Lead Tri-Halide Perovskites. *Nat. Commun.* **2014**, *5*, 3586.

(28) Xiao, Z.; Bi, C.; Shao, Y.; Dong, Q.; Wang, Q.; Yuan, Y.; Wang, C.; Gao, Y.; Huang, J. Efficient, High Yield Perovskite Photovoltaic Devices Grown by Interdiffusion of Solution-Processed Precursor Stacking Layers. *Energy Environ. Sci.* **2014**, *7*, 2619.

(29) Yang, J.; Siempelkamp, B. D.; Liu, D.; Kelly, T. L. Investigation of $\text{CH}_3\text{NH}_3\text{PbI}_3$ Degradation Rates and Mechanisms in Controlled Humidity Environments Using in Situ Techniques. *ACS Nano* **2015**, *9*, 1955–1963.

(30) Zheng, L.; Ma, Y.; Chu, S.; Wang, S.; Qu, B.; Xiao, L.; Chen, Z.; Gong, Q.; Wu, Z.; Hou, X. Improved Light Absorption and Charge Transport for Perovskite Solar Cells with Rough Interfaces by Sequential Deposition. *Nanoscale* **2014**, *6*, 8171–8176.

(31) Eperon, G. E.; Burlakov, V. M.; Goriely, A.; Snaith, H. J. Neutral Color Semitransparent Microstructured Perovskite Solar Cells. *ACS Nano* **2014**, *8*, 591–598.

(32) Sun, S.; Salim, T.; Mathews, N.; Duchamp, M.; Boothroyd, C.; Xing, G.; Sum, T. C.; Lam, Y. M. The Origin of High Efficiency in Low-Temperature Solution-Processable Bilayer Organometal Halide Hybrid Solar Cells. *Energy Environ. Sci.* **2014**, *7*, 399–407.

(33) Wehrenfennig, C.; Liu, M.; Snaith, H. J.; Johnston, M. B.; Herz, L. M. Homogeneous Emission Line Broadening in the Organo Lead Halide Perovskite $\text{CH}_3\text{NH}_3\text{PbI}_{3-x}\text{Cl}_x$. *J. Phys. Chem. Lett.* **2014**, *5*, 1300–1306.